Novelty Journals

ISSN 2394-9716

International Journal of Novel Research in Interdisciplinary Studies
Vol. 10, Issue 2, pp: (1-15), Month: March – April 2023, Available at: www.noveltyjournals.com

Magnetic Induction Effects on Unsteady MHD Nanofluid Flow Past an Oscillating Semi-Infinite Vertical Flat Plate Embedded in Porous Media

[1]Rhoda King'ali, [2]Mark Kimathi, [3]Benjamin Kikwai

[1]Mathematics & Statistics, Machakos University, Machakos, Kenya

[2]Mathematics & Statistics, Machakos University, Machakos, Kenya

[3]Mathematics & Statistics, Machakos University, Machakos, Kenya

DOI: https://doi.org/10.5281/zenodo.7687861

Published Date: 01-March-2023

Abstract: **This research work addresses the effects of induced magnetic field and thermal diffusion for an incompressible, unsteady, viscous MHD Nano-fluid flow past a semi-infinite oscillating vertical flat plate embedded in a porous media. A strong magnetic field is subjected transversely to the direction of the flow. The Partial differential equations governing the flow, together with boundary and initial conditions, are solved by finite difference method of approximation. Numerical simulation has been done by use MATLAB software. The effects of the flow parameters on temperature, velocity, and concentration profiles have been investigated, discussed and results presented in graphs. It is found that an increase in magnetic Reynolds number and Reynolds number causes an increase in the induced magnetic field and decreases the induced magnetic field far away from the plate. This leads to decrease in concentration due to increase in inertial forces hence an increase in temperature and velocity**

Keywords: **Induced Magnetic Field, Chemical Reaction, MHD, Nanofluid, Rotation.**

I. INTRODUCTION

MHD convective heat transfer in Nano-fluids has many applications and participates in an essential task in both sciences and engineering. They need heat transfer fluids in technology for applications such as cooling or heating, solar energy, and nuclear reactors, among others. Since fluids have a lower thermal conductivity than metals, it is essential to combine all types of fluids with Nano-sized metals to improve the fluids' heat transfer capacity. In this regard, the study of Nano-fluids has received extensive attention in the past decade due to enormous industrial, transportation, electronics, biomedical applications, such as in advanced nuclear systems, cylindrical heat pipes, automobiles, fuel cells, drug delivery, biological sensors, and hybrid-powered engines. Nano-fluid is a term initially used by [1] and refers to a new class of heat transfer fluids with superior thermal properties. The mixture of the base fluid and nanoparticles having unique physical and chemical properties is referred to as a Nano-fluid. It is expected that the presence of the nanoparticles in the Nano-fluid increases the thermal conductivity and therefore substantially enhances the heat transfer characteristics of the Nano-fluid. [2] Studied on Thermal-diffusion and diffusion-thermo effects on MHD flow through porous medium past an exponentially accelerated inclined plate with variable temperature. They used a robust finite element method (FEM) to obtain the solution of the transformed modeled flow equations with initial and boundary conditions. [3] Researched on the effects of thermal diffusion and joule heating on MHD radiative and convective casson fluid flow past oscillating semi-infinite vertical porous plate. They used finite difference method of approximation to solve the partial differential equations which governed the flow. [4] Diffusion thermo and thermal diffusion effects on MHD free convection flow of Rivlin-Ericksen fluid past a semi-infinite vertical plate with viscous dissipation considered. They used finite difference method of approximation to solve the non-linear systems of partial differential equations governing the flow. [5] Researched on Magneto-hydrodynamics (MHD) Heat and Mass Transfer of Casson Fluid Flow Past a Semi-Infinite Vertical Plate with thermophoresis effect. The spectral relaxation method (SRM) was used to numerically solve the modeled equations governing the flow. [6] Studied effect of thermal diffusion and heat-generation on MHD nanofluid flow past an oscillating vertical plate through porous medium. They used Laplace transform to solve the system of partial differential equations. [7] Studied radiation-absorption, chemical reaction, and Hall and ion-slip impacts on unsteady MHD free convective laminar flow of an incompressible viscous, electrically conducting and heat generation /absorbing fluid enclosed with a semi-infinite porous plate within a rotating frame. They used harmonic and non-harmonic functions to analytically solve the non-dimensional governing equations. Keeping the above into consideration, we consider effects of induced magnetic field and thermal diffusion on MHD flow of nanofluid past an oscillatory vertical flat plate embedded in a porous media

II. MATHEMATICAL FORMULATION

This study considers free convective, radiative and a one dimensional (1-D) magneto hydrodynamic laminar fluid flow past an oscillating semi-infinite vertical porous plate subjected to a uniform magnetic field. The $x-axis$ is at the vertically upward direction which is the direction of flow. The $z-axis$ is taken normal to the plate.

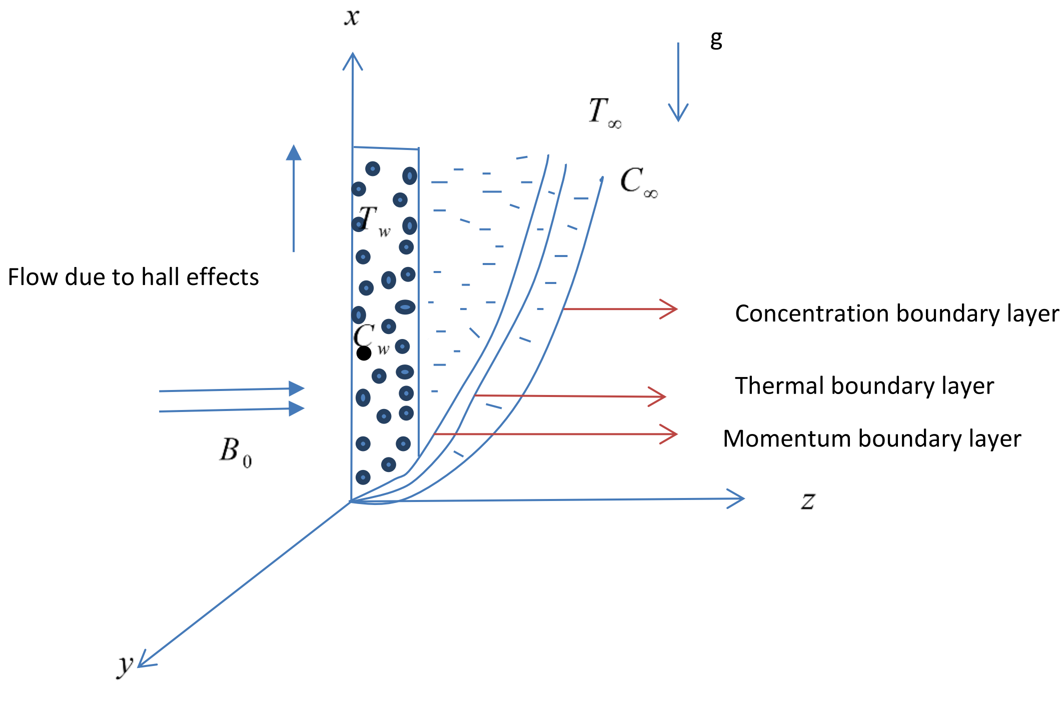

MODEL ASSUMPTIONS

It is assumed that the only significant body forces are Lorentz and gravitational forces, the chemical reaction between the fluid and nanoparticles is negligible, the nanofluid is considered electrically conducting, coefficient of viscosity is constant, the induced magnetic field is taken to be strong, and all the variables are functions of $z \text{ and } t$ only. Considering the above assumptions the equations of continuity, momentum, energy, concentration and magnetic induction governing the flow are as follows:

International Journal of Novel Research in Interdisciplinary Studies
Vol. 10, Issue 2, pp: (1-15), Month: March – April 2023, Available at: www.noveltyjournals.com

III. EQUATIONS GOVERNING THE FLOW

CONTINUITY EQUATION

$$\frac{\partial w}{\partial z} = 0 \tag{1}$$

EQUATION OF MOMENTUM

Under the Boussinesq approximation and neglecting the pressure gradient as well as considering the oscillatory motion given by [8] and that the fluid velocity through porous media is approximately inversely proportional to the kinematic viscosity of the fluid , μ_{nf} , the momentum equations are given as;

$$\rho_{nf}\left[\frac{\partial v}{\partial t}+\frac{\partial u}{\partial z}-2\Omega v\right]=\mu_{nf}\left[\frac{\partial^2 u}{\partial z^2}\right]-\frac{\mu_{nf}}{k}u+g\rho_{nf}\left[(\beta_T)_{nf}(T-T_\infty)+(\beta_C)_{nf}(C-C_\infty)\right] + B_0\vec{J}_y \tag{2}$$

$$\rho_{nf}\left[\frac{\partial v}{\partial t}+\frac{\partial v}{\partial z}-2\Omega u\right]=\mu_{nf}\left[\frac{\partial^2 v}{\partial z^2}\right]-\frac{\mu_{nf}}{k}v+g\rho_{nf}\left[(\beta_T)_{nf}(T-T_\infty)+(\beta_C)_{nf}(C-C_\infty)\right] + b\vec{J}_z - B_0\vec{J}_x \tag{3}$$

The boundary and initial conditions are specified as;

$$For\ t \le 0;\ u = v = 0;\ T = T_\infty;\ C = C_\infty \quad for\ \ all\ \ z$$

$$At\ t > 0 and\ z = 0;\ v = 0; u = U_r(1+\varepsilon\cos t);\ \frac{\partial T}{\partial z} = -\frac{h_f}{k_{nf}}(T_w - T_\infty);\ \frac{\partial C}{\partial z} = -\frac{h_s}{D_B}(C_w - C_\infty) T = T_\infty;$$

$$For\ t > 0;\ u \to 0,\ v \to 0;\ T \to T_\infty;\ C \to C_\infty \quad as\ z \to \infty$$

Where U_r is the uniform velocity and ε is a small constant quantity.

However the magnetic field strength are presumed to be very small and the generalized Ohm's law is adapted with Hall impacts excluded.

$$J + \frac{w_e \tau_e}{B_0}[J \times B] = \sigma\left[E + V \times B + \frac{1}{e\eta_e}\vec{\nabla}\rho_e\right] \tag{4}$$

Using the assumption that there are no externally applied electric field that is; $\vec{E} = 0$ (short-circuit problem) and neglecting the electronic pressure; $\frac{1}{e\eta_e}\vec{\nabla}\rho_e = 0$ we have;

$$J = \sigma[V \times B] \tag{5}$$

where;

$$\vec{V} = ui + vj + wk \ \text{ and } \ \vec{B} = bi + 0j + B_0 k \tag{6}$$

Putting into consideration the above assumptions and with exclusion of Hall effects, equation (5) yields;

$$J_x = \delta B_0 v \tag{7}$$

$$J_y = -\delta B_0 u \tag{8}$$

$$J_z = -\delta b v \tag{9}$$

Substituting (7), (9) and (8) into (2) and (3) accordingly we get;

$$\rho_{nf}\left\{\frac{\partial u}{\partial t} + w\frac{\partial u}{\partial z} - 2\Omega v\right\} = \mu_{nf}\left\{\frac{\partial^2 u}{\partial z^2}\right\} - \frac{\mu_{nf}}{k}u + g\rho_{nf}\left\{(\beta_T)_{nf}(T - T_\infty) + (\beta_C)_{nf}(C - C_\infty)\right\} - \delta B_0^2 u \tag{10}$$

$$\rho_{nf}\left\{\frac{\partial v}{\partial t} + w\frac{\partial v}{\partial z} + 2\Omega u\right\} = \mu_{nf}\left\{\frac{\partial^2 v}{\partial z^2}\right\} - \frac{\mu_{nf}}{k}v + g\rho_{nf}\left\{(\beta_T)_{nf}(T - T_\infty) + (\beta_C)_{nf}(C - C_\infty)\right\} + \delta B_0^2 v \tag{11}$$

EQUATION OF ENERGY

In this study, thermal radiation is considered as a significant energy source, S_e. Additionally, the porous plate is in presence of thermal buoyancy effect with constant heat source and convective boundary condition.

According to [9] thermal diffusivity α_{nf} of nanofluid is given as; $\alpha_{nf} = \dfrac{k_{nf}}{(\rho C_p)_{nf}}$ therefore the energy equation becomes;

$$\frac{\partial T}{\partial t} + w\frac{\partial T}{\partial z} = \alpha_{nf}\left(\frac{\partial^2 T}{\partial z^2}\right) + \frac{Q}{(\rho C_p)_{nf}}(T - T_\infty) - \frac{\partial q}{\partial z} \tag{12}$$

Where Q is temperature dependent volumetric rate of heat source. The radiative heat transfer is catered for by Stefan-Boltzmann law of radiation which advocates that the total radiative energy emitted by a black body is directly proportional to the fourth power of its temperature. Using the Rosseland approximation given by [10] the radiative heat flux is expressed as;

$$\frac{\partial q_r}{\partial z} = -\frac{16\sigma^* T_\infty^{\,3}}{3k^*}\frac{\partial^2 T}{\partial z^2} \tag{13}$$

Where $\sigma^*\left(= 5.67 \times 10^{-8} \quad W/m^2k^4\right)$ is the Stefan-Boltzmann constant and $k^*\left(m^{-1}\right)$ is the Rosseland mean absorption coefficient.

EQUATION OF NANOPARTICLE CONCENTRATION

$$\frac{\partial C}{\partial t} + w\frac{\partial C}{\partial z} = D_B\left(\frac{\partial^2 C}{\partial z^2}\right) + k'(C - C_\infty) \tag{14}$$

Where, D_B is the diffusivity constant and k' is the chemical reaction constant.

EQUATION OF MAGNETIC INDUCTION

$$\frac{\partial b}{\partial t} = -v\frac{\partial b}{\partial z} - w\frac{\partial b}{\partial z} + B_0\frac{\partial u}{\partial z} + D_m\frac{\partial^2 b}{\partial z^2} \tag{15}$$

International Journal of Novel Research in Interdisciplinary Studies
Vol. 10, Issue 2, pp: (1-15), Month: March – April 2023, Available at: www.noveltyjournals.com

Nano-fluids possess various thermo-physical properties which include; specific heat capacity, electrical conductivity, dynamic viscosity, thermal conductivity, density and coefficient of volume expansion due to changes in temperature and concentration. According to [9] the following are thermo-physical characteristics of nanofluids where f denote H_2O , s denote Al_2O_3 and ϕ is the solid volume fraction of the nanoparticles.

The density of the nanofluid;

$$\rho_{nf} = (1-\phi)\rho_f + \phi\rho_s \tag{16}$$

The specific heat capacity of the nano-fluid;

$$(\rho C_P)_{nf} = (1-\phi)(\rho C_p)_f + \phi(\rho C_p)_s \tag{17}$$

The thermal conductivity of the nano-fluid;

$$\frac{k_{nf}}{k_f} = \left[\frac{k_s + 2k_f - 2\phi(k_f - k_s)}{k_s + 2k_f + \phi(k_f - k_s)}\right] \tag{18}$$

The dynamic viscosity of the nano-fluid;

$$\mu_{nf} = \frac{\mu_f}{(1-\phi)^{2.5}} \tag{19}$$

The volume coefficient as a result of temperature changes of the nano-fluid;

$$(\beta_T)_{nf} = (1-\phi_s)(\beta_T)_f + \phi_s(\beta_T)_s \tag{20}$$

In a similar manner the volume expansion coefficient as a result of concentration change of the nano-fluid;

$$(\beta_C)_{nf} = (1-\phi_s)(\beta_C)_f + \phi_s(\beta_C)_s \tag{21}$$

Introducing the non-dimensional quantities;

$$u^* = \frac{u}{U_r};\quad v^* = \frac{v}{U_r};\quad z^* = \frac{z}{L};\quad t^* = \frac{tU_r}{L};\quad b^* = \frac{b}{B_0}$$

$$\psi = \frac{C - C_\infty}{C_w - C_\infty};\quad \theta = \frac{T - T_\infty}{T_w - T_\infty};\quad R = \frac{2\Omega v_f}{U_r^2};\quad P_r = \frac{v_f}{\alpha_f};\quad S = \frac{w_0}{U_r};\ K_r = \frac{Lk'}{U_r}$$

$$K = \frac{kU_r}{v_f L};\quad Q_H = \frac{Qv_f^2}{U_r^2 k_f};\quad M^2 = \frac{\delta_f B_0^2 L}{\rho_{nf} U_r};\quad S_c = \frac{v}{D_B};\quad G_r = \frac{\vec{g}(\beta_T)_{nf}(T_w - T_\infty)L}{U_r^2}$$

$$G_c = \frac{\vec{g}(\beta_C)_{nf}(C_w - C_\infty)L}{U_r^2}\quad R_m = \frac{U_r L}{D_m},\ R_e = \frac{U_r L}{v_f}$$

Where R is the Rotation parameter, S is the Suction parameter, P_r is the Prandtl number, K is the permeability parameter, M is the magnetic field parameter, Q_H is the heat source parameter, K_r is the chemically reacting parameter and S_c is the Schmidt's quantity, F is the thermic dissipation parameter, R_m is the magnetic Reynolds number, G_r *and* G_c are Grashof numbers and R_e is Reynolds number.

International Journal of Novel Research in Interdisciplinary Studies
Vol. 10, Issue 2, pp: (1-15), Month: March – April 2023, Available at: www.noveltyjournals.com

In this study, all the variables without superscript $\left(^{*}\right)$ star represent dimensional variables, otherwise non-dimensional variables.

According to Das (2014) the continuity equation (1) reduces to;

$$w = w_0 \tag{22}$$

Where w_0 is the normal velocity at the plate which is negative for suction and positive for injection.

Making use of the forementioned non-dimensionalized quantities and nanoparticle thermo-physical characteristics, equations (10), (11), (12), (14), and (15) reduces to;

$$\begin{aligned}\left[1-\phi+\phi\left(\frac{\rho_s}{\rho_f}\right)\right]\left(\frac{\partial u^*}{\partial t^*}+S\frac{\partial u^*}{\partial z^*}-RR_e v^*\right) &= \frac{1}{(1-\phi)^{2.5}}\frac{1}{R_e}\frac{\partial^2 u^*}{\partial z^{*2}}-\frac{1}{(1-\phi)^{2.5}}\frac{1}{K}u^* \\ &+\left[1-\phi+\phi\left(\frac{\rho_s}{\rho_f}\right)\right](G_r\theta+G_c\psi) \\ &-\left(1-\phi+\phi\left(\frac{\rho_s}{\rho_f}\right)\right)M^2u^*-\left(1-\phi+\phi\left(\frac{\rho_s}{\rho_f}\right)\right)M^2Sb^*\end{aligned} \tag{23}$$

$$\begin{aligned}\left[1-\phi+\phi\left(\frac{\rho_s}{\rho_f}\right)\right]\left(\frac{\partial v^*}{\partial t^*}+S\frac{\partial v^*}{\partial z^*}-RR_e u^*\right) &= \frac{1}{(1-\phi)^{2.5}}\frac{1}{R_e}\frac{\partial^2 v^*}{\partial z^{*2}}-\frac{1}{(1-\phi)^{2.5}}\frac{1}{K}v^* \\ &+\left[1-\phi+\phi\left(\frac{\rho_s}{\rho_f}\right)\right](G_r\theta+G_c\psi) \\ &+\left(1-\phi+\phi\left(\frac{\rho_s}{\rho_f}\right)\right)M^2\left[-b^{*2}v^*-v^*\right]\end{aligned} \tag{24}$$

$$\left[1-\phi+\phi\left(\frac{(\rho C_P)_s}{(\rho C_P)_f}\right)\right]\left(\frac{\partial\theta}{\partial t^*}+S\frac{\partial\theta}{\partial z^*}\right)=\frac{1}{P_r}\frac{1}{R_e}\frac{\partial^2\theta}{\partial z^{*2}}+Q_H\theta+\frac{4}{3}\frac{F}{R_e}\frac{\partial^2\theta}{\partial z^{*2}} \tag{25}$$

$$\frac{\partial\psi}{\partial t^*}+S\frac{\partial\psi}{\partial z^*}=\frac{1}{S_c}\frac{1}{R_e}\frac{\partial^2\psi}{\partial z^{*2}}+K_r\psi \tag{26}$$

$$\frac{\partial b^*}{\partial t^*}=S\frac{\partial b^*}{\partial z^*}+\frac{\partial u^*}{\partial z^*}+\frac{1}{R_e}\frac{\partial^2 b^*}{\partial z^{*2}} \tag{27}$$

The transformed boundary and initial conditions are;

$$For\ t\le 0;\ u^*=v^*=0;\ \theta=0;\ \psi=0\quad for\ \ all\ z$$

$$For\ t>0\ and\ \ z=0;\ u=U_r(1+\varepsilon\cos t);\ v=0,\ \frac{\partial\theta}{\partial z^*}=-N_c(1-\theta(z)),\ \frac{\partial\psi}{\partial z^*}=-N_d(1-\psi(z))$$

$$For\ t>0;\ u=v=0;\ \theta\to 0;\ \psi\to 0\ as\ z\to\infty$$

International Journal of Novel Research in Interdisciplinary Studies
Vol. 10, Issue 2, pp: (1-15), Month: March – April 2023, Available at: www.noveltyjournals.com

METHOD OF SOLUTION

In order to solve equations (22) to (27), the finite difference method has been used, due to the following merits;

1.) Finite difference method is convergent. When you increase or reduce the step size the solution tends to the exact solution.

2.) It is consistent. The truncation error tends to zero as the step size decreases.

3.) It is stable. The effect of the round off error remains bounded as the mesh points tend to infinity with fixed sizes.

However, we acknowledge that there are other more efficient methods, which are beyond the scope of this present study.

$$u^{*n+1}_{i} = \Delta t\left\{ \begin{array}{l} S\left[\dfrac{u^{*n}_{k+1}-u^{*n}_{k-1}}{2\Delta z}\right] + Rv^{*n}_{i,k} + \dfrac{1}{(1-\phi)^{2.5}\left(1-\phi+\phi\left(\dfrac{\rho_s}{\rho_f}\right)\right)}\dfrac{1}{R_e}\left(\dfrac{u^{*n}_{k+1}-2u^{*n}_{k}+u^{*n}_{k-1}}{(\Delta z)^2}\right) - \\ \dfrac{1}{(1-\phi)^{2.5}\left(1-\phi+\phi\left(\dfrac{\rho_s}{\rho_f}\right)\right)}\dfrac{1}{K}u^{*n}_{i,k} + \left(G_r\theta^{n}_{i,k}+G_c\psi^{n}_{i,k}\right) - M^2u^{*\,n}_{i,k} - M^2Sb^{*\,n}_{i,k} \end{array} \right\} + u^{*n}_{i} \qquad (28)$$

$$v^{*n+1}_{i} = \Delta t\left\{ \begin{array}{l} S\left[\dfrac{v^{*n}_{k+1}-v^{*n}_{k-1}}{2\Delta z}\right] + Ru^{*n}_{i,k} + \dfrac{1}{(1-\phi)^{2.5}\left(1-\phi+\phi\left(\dfrac{\rho_s}{\rho_f}\right)\right)}\dfrac{1}{R_e}\left(\dfrac{v^{*n}_{k+1}-2v^{*n}_{k}+v^{*n}_{k-1}}{(\Delta z)^2}\right) - \\ \dfrac{1}{(1-\phi)^{2.5}\left(1-\phi+\phi\left(\dfrac{\rho_s}{\rho_f}\right)\right)}\dfrac{1}{K}v^{*n}_{i,k} + \left(G_r\theta^{n}_{i,k}+G_c\psi^{n}_{i,k}\right) + M^2\left(\dfrac{-b^{*2n}_{i,k}v^{*n}_{i,k}-v^{*n}_{i,k}}{1}\right) \end{array} \right\} + u^{*n}_{i} \qquad (29)$$

$$\theta^{n+1}_{i} = \Delta t\left\{ S\left(\frac{\theta^{n}_{k+1}-\theta^{n}_{k-1}}{2\Delta z}\right) + \frac{1}{1-\phi+\phi\left(\dfrac{(\rho\beta)_s}{(\rho\beta)_f}\right)}\left[\begin{array}{l} \dfrac{1}{P_rR_e}\left(\dfrac{\theta^{n}_{k+1}-2\theta^{n}_{k}+\theta^{n}_{k-1}}{(\Delta z)^2}\right) + \\ Q_H\theta^{n}_{i,k} + \dfrac{4}{3}\dfrac{F}{R_e}\left(\dfrac{\theta^{n}_{k+1}-2\theta^{n}_{k}+\theta^{n}_{k-1}}{(\Delta z)^2}\right) \end{array} \right] \right\} + \theta^{n}_{i,k} \qquad (30)$$

$$\psi^{n+1}_{i} = \Delta t\left\{ S\left[\frac{\psi^{n}_{k+1}-\psi^{n}_{k-1}}{2\Delta z}\right] + \frac{1}{S_cR_e}\left[\frac{\psi^{n}_{k+1}-2\psi^{n}_{k}+\psi^{n}_{k-1}}{(\Delta z)^2}\right] + K_r\psi^{n}_{i,k} \right\} + \psi^{n}_{i} \qquad (31)$$

$$b^{*n+1}_{i} = \Delta t\left\{ -v^{*}\left[\frac{b^{*n}_{k+1}-b^{*n}_{k-1}}{2\Delta z}\right] + S\left[\frac{b^{*n}_{k+1}-b^{*n}_{k-1}}{2\Delta z}\right] - \left[\frac{u^{*n}_{k+1}-u^{*n}_{k-1}}{2\Delta z}\right] + \frac{R_m}{R_e}\left[\frac{b^{*n}_{k+1}-2b^{*n}_{k}+b^{*n}_{k-1}}{(\Delta z)^2}\right] \right\} + b^{*n}_{i} \qquad (32)$$

The discretized initial and boundary conditions:

$$For\ \ t \le 0;\ \ u^{*n}_{i,k} = v^{*n}_{i,k} = 0;\ \ \theta^{n}_{i,k} = 0;\ \ \psi^{n}_{i,k} = 0\ \ \ for\ \ all\ \ k$$

$$For\ \ t > 0\ \ and\ \ k = 0;\ u^{*n}_{i,k} = U_r(1+\varepsilon\cos t);\ v^{*n}_{i,k} = 0,$$
$$\theta^{n}_{k+1} = -N_c\left(1-\theta^{n}_{i,k}\right)2\Delta z + \theta^{n}_{k=1},\ \psi^{n}_{k+1} = -N_d\left(1-\psi^{n}_{i,k}\right)2\Delta z + \psi^{n}_{k-1}$$

$$For\ \ t > 0;\ \ u^{*n}_{i,k} = v^{*n}_{i,k} = 0;\ \ \theta^{n}_{i,k} \to 0;\ \ \psi^{n}_{i,k} \to 0\ \ \ as\ \ k \to \infty$$

Novelty Journals

ISSN 2394-9716

International Journal of Novel Research in Interdisciplinary Studies
Vol. 10, Issue 2, pp: (1-15), Month: March – April 2023, Available at: www.noveltyjournals.com

IV. RESULTS AND DISCUSSIONS

The following parameter values are used throughout the numerical solution process except where otherwise stated, $\phi = 0.35$, $\rho_s = 3950$, $\rho_f = 997$, $(C_p)_s = 765$, $(C_p)_f = 4179$, $R = 0.015$, $S = -0.2$, $K = 0.8$, $m = 0.7$, $M = 2$, $G_r = 1.5$, $G_c = 1.5$, $S_c = 0.8$, $K_r = 2$, $R_m = 65$, $R_e = 180$, $N_c = 1$, $N_d = 1$, $P_r = 6.72$, $Q_H = 2.5$, $F = 0.6$

i. Effects of flow parameters on velocity profiles

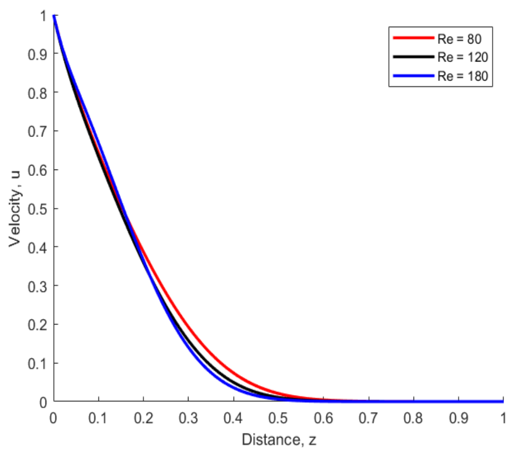

Fig. 1. primary velocity and Reynolds Number, R_e

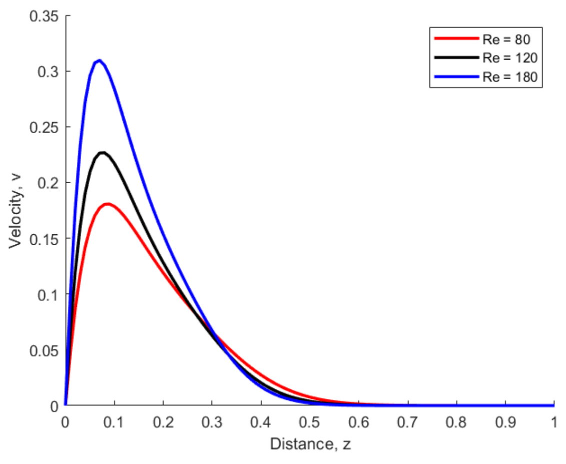

Fig. 2. Secondary velocity and Reynolds Number, R_e

From Fig. 1 & 2, it is observed that;

An increase in the Reynolds Number leads to an increase in both primary and secondary velocities near the plate but decreases the velocity away from the plate to a point where the velocity becomes uniformly distributed. This is because increase in Reynolds number means the viscous force becomes less predominant hence the inertia forces prevails.

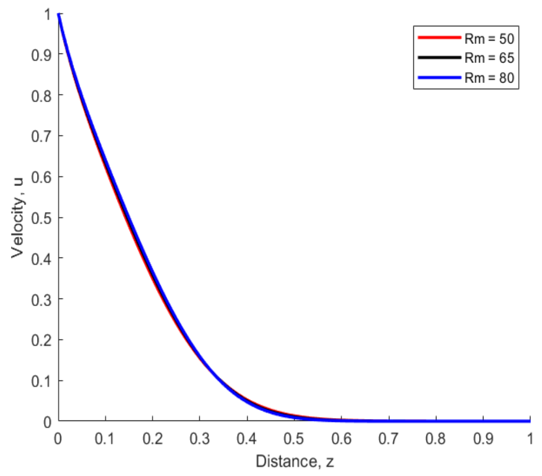

Fig. 3. primary velocity and maganetic Reynolds number, R_m

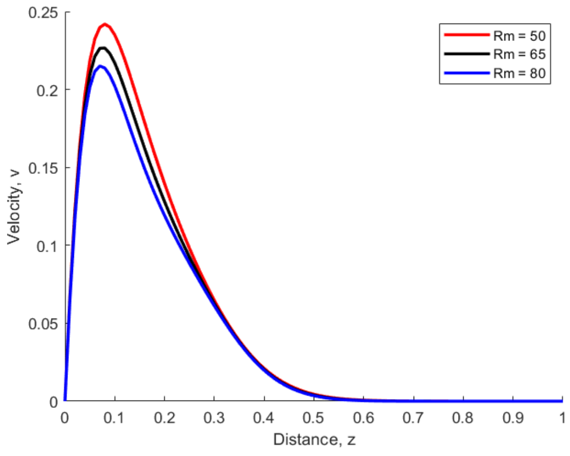

Fig. 4. secondary velocity and Magnetic Reynolds number, R_m

International Journal of Novel Research in Interdisciplinary Studies
Vol. 10, Issue 2, pp: (1-15), Month: March – April 2023, Available at: www.noveltyjournals.com

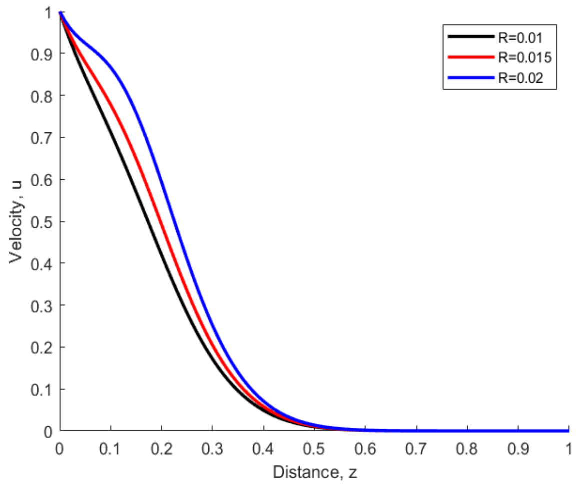

Fig. 5. primary velocity and rotation parameter, R

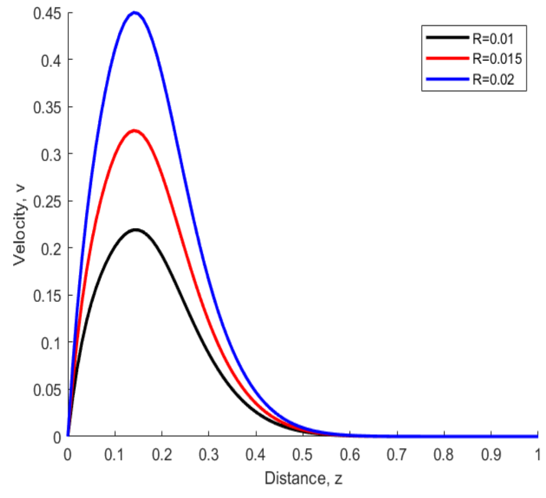

Fig. 6. secondary velocity and rotation parameter, R

From Fig. 5 & 6; we note that;

Increase in the rotation parameter, R increases both primary and secondary velocities near the plate and remains constantly distributed far away from the plate. This is due to increase in Coriolis force on velocity of the rotating fluid hence increase in velocity.

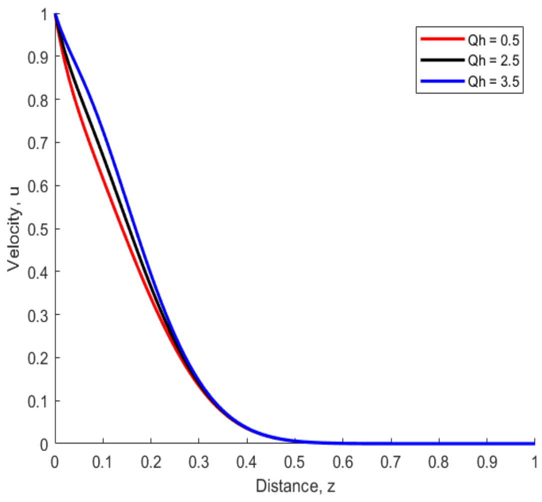

Fig. 7. primary velocity and heat source parameter, Q_h

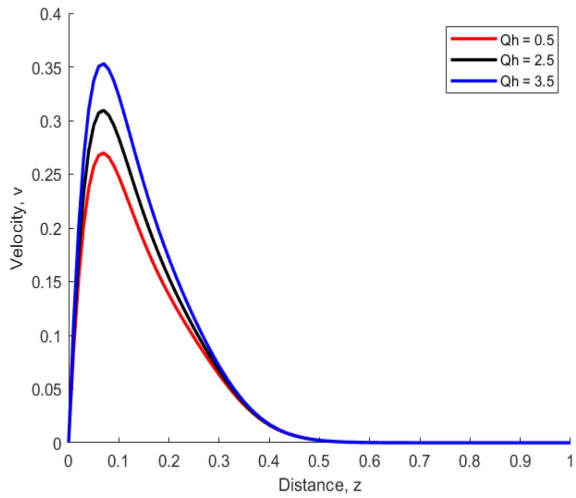

Fig. 8. primary velocity and heat source parameter, Q_h

From Fig. 7 and 8, we note that;

An increase in the heat source parameter, Q_h increases both primary and secondary velocities near the plate and remains constantly distributed far away from the plate. Increase in heat source means increase in temperature gradient and this leads to increase in velocity distributions.

International Journal of Novel Research in Interdisciplinary Studies
Vol. 10, Issue 2, pp: (1-15), Month: March – April 2023, Available at: www.noveltyjournals.com

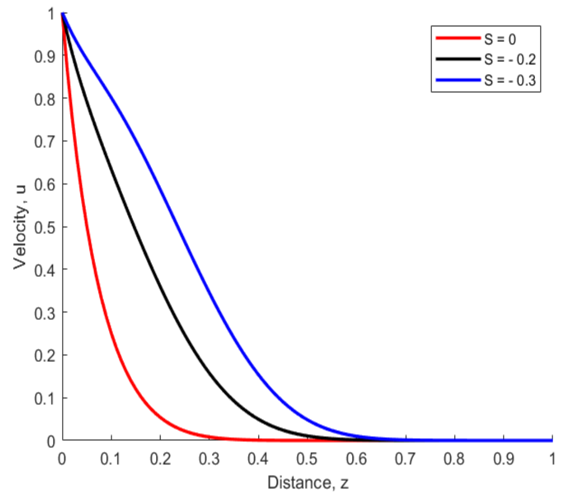

Fig. 9. primary velocity and Suction Parameter, S

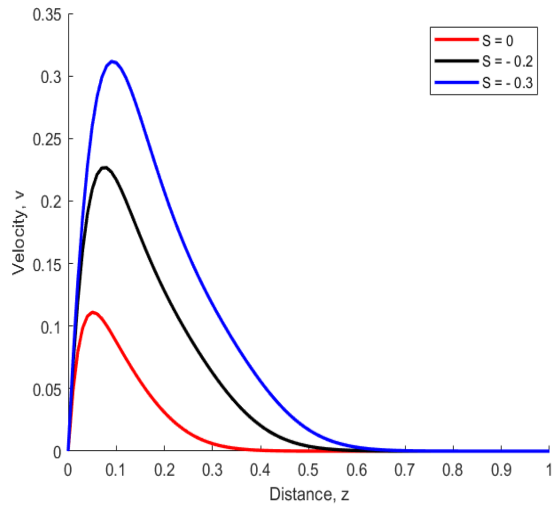

Fig. 10. secondary velocity and Suction Parameter, S

From Fig. 9 and 10; we observe that;

Increase in the suction parameter increases both primary and secondary profiles near the plate and the velocities remain constant far away from the plate. This is because increase in suction leads to suction pressure which creates a low pressure region which makes the fluid to flow faster to fill the lower pressure region hence an increase velocity.

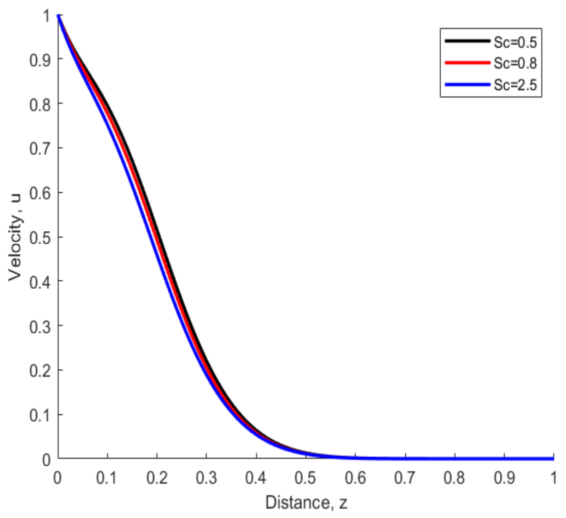

Fig. 11. primary velocity and Schmidt number, S_c

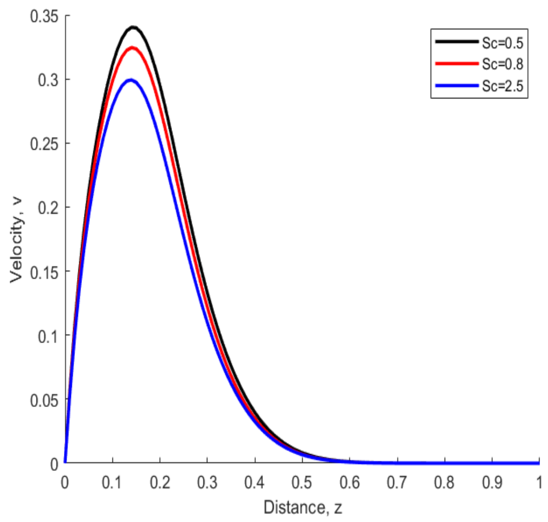

Fig. 12. secondary velocity and Schmidt number, S_c

From the Fig. 11 & 12; we note that;

An increase in the mass diffusion parameter, S_c leads to a decrease in both primary and secondary velocity profiles near the plate and remain constantly distributed far away from the plate. This is due to increase in viscous diffusion rate which leads to decrease in buoyancy forces; which in turn results to reduction in flow of the fluid.

ii. Effects of Flow Parameter on Temperature Profiles

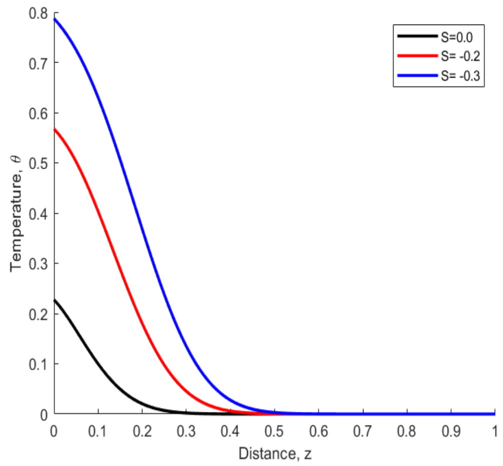

Fig. 13. Temperature and suction parameter, S

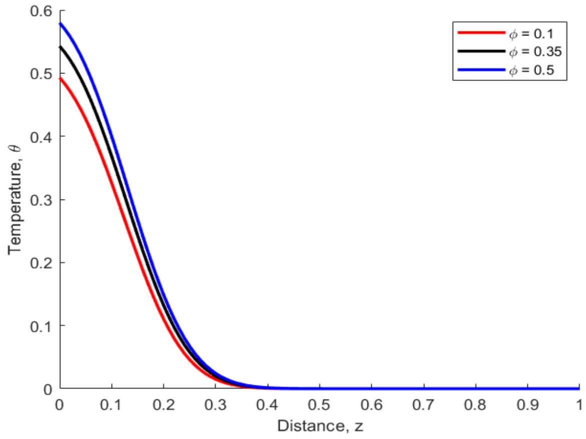

Fig. 14. Temperature and specification of volume fractions of nanoparticles, ϕ

From the Fig. 13 and 14; we note that;

- A decrease in the suction parameter, S increases the temperature profiles. This is because suction leads to increase in velocities which further leads to the increase in the kinetic energy which is converted in to thermal energy and this results to temperature increase.
- Increasing the volume fractions of nanoparticles, ϕ causes an increase in the temperature profiles. This is as a result of increase in the thermal boundary layer thickness.

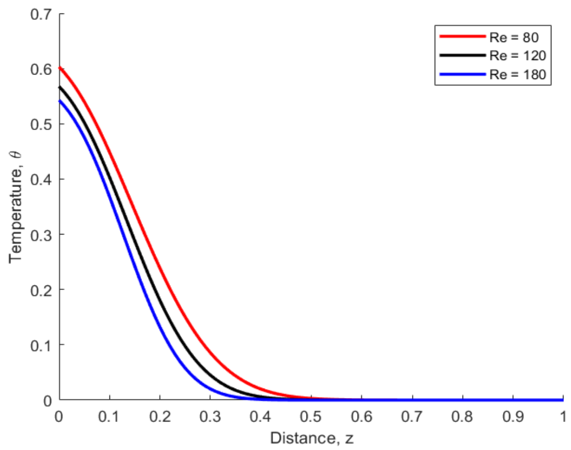

Fig. 15. Temperature and Reynolds number, R_e

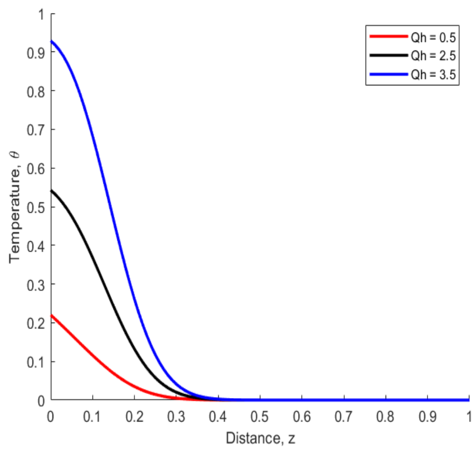

Fig. 16. Temperature and heat source parameter, Q_h

From Fig. 15 & 16, it is noted that;

- An increase in Reynolds number, R_e increases the temperature profiles. This is due to decrease in viscous forces and since temperature and viscosity are inversely proportional, a decrease in viscous forces yields an increase in temperature.
- Increasing the heat source parameter leads to an increase in temperature.

International Journal of Novel Research in Interdisciplinary Studies
Vol. 10, Issue 2, pp: (1-15), Month: March – April 2023, Available at: www.noveltyjournals.com

iii. Effects of Flow Parameters on Concentration Profiles

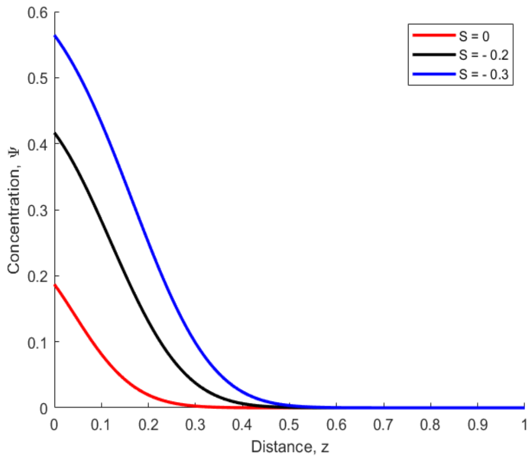

Fig. 17. concentration and suction parameter, S

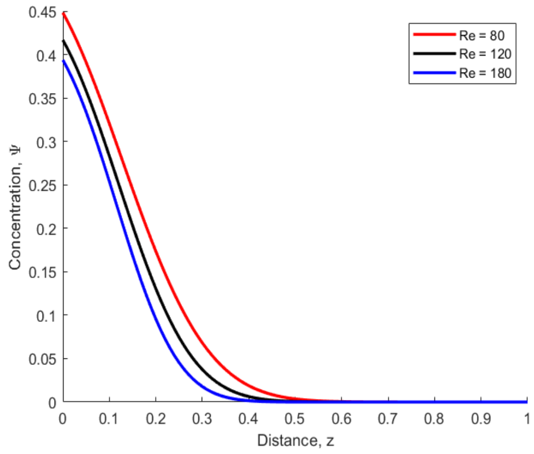

Fig. 18. Concentration and Reynolds number, R_e

From the Fig. 17 and 18; we note that;

- Decreasing the suction parameter, S increases the concentration. This is due to high temperatures as a result of increased kinetic energy hence a decrease in concentration boundary layer.

- An increase in the Reynolds number, R_e leads to a decrease in the concentration profiles due to increase in inertial forces which increases the velocity hence a decrease in concentration.

iv. Effects of Flow Parameters on induced magnetic field Profiles

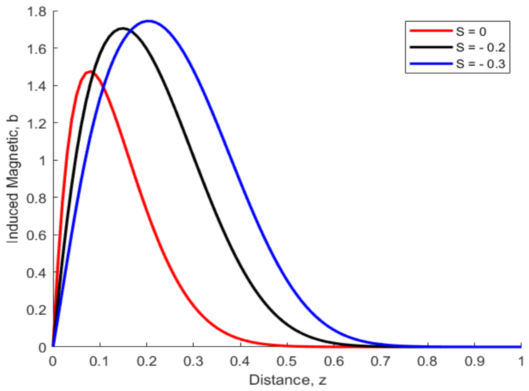

Fig. 19. Induced magnetic field and Suction, S

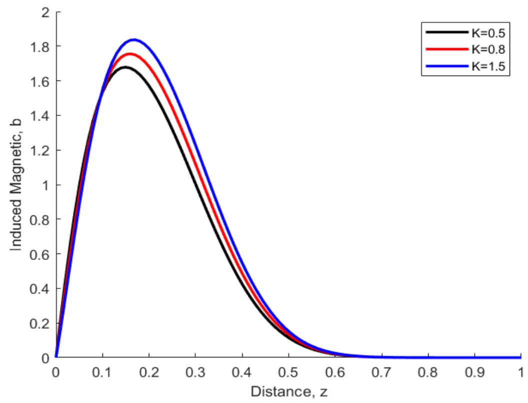

Fig. 20. Induced magnetic field and permeability parameter, K

From Fig. 19 & 20 we note that;

- Reducing the Suction parameter diminishes the induced magnetic field profiles near the plate and increases the induced magnetic far away from the plate. This is because with decrease in suction parameter, the velocity decreases hence a decrease in interaction between the magnetic field and the fluid leading to a decreased magnetic induction.

- An increase in the Permeability parameter, K causes an increase in the induced magnetic field near the plate and decreases the induced magnetic field far away from the plate.

International Journal of Novel Research in Interdisciplinary Studies
Vol. 10, Issue 2, pp: (1-15), Month: March – April 2023, Available at: www.noveltyjournals.com

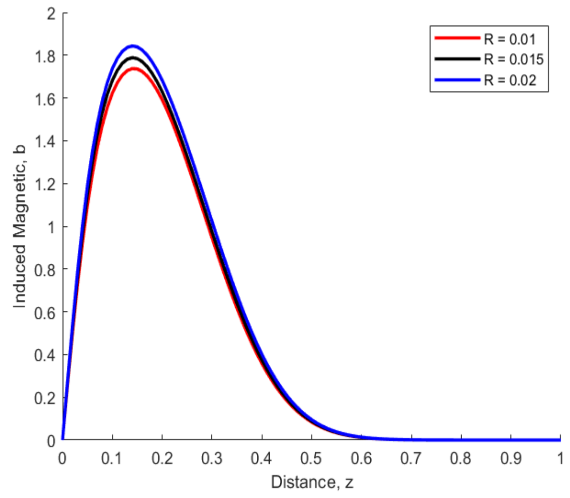

Fig. 21. Induced magnetic field and Rotation parameter, R

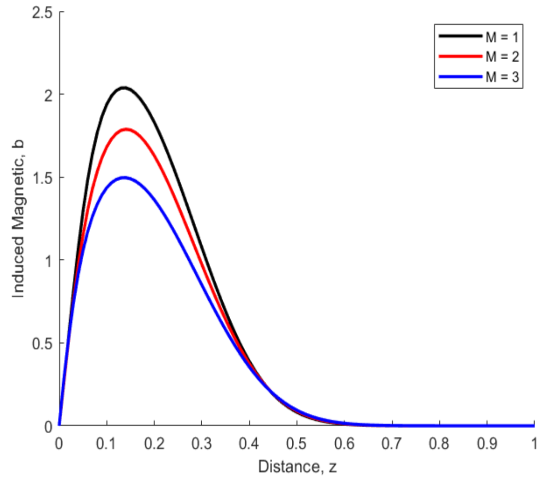

Fig. 22. Induced magnetic field and magnetic field parameter, M

From Fig. 21 & 22, we observe that;

- The induced magnetic field increases with an increase in rotation parameter, R . This is as a result increased magnetic field which induces electromotive force hence the faster the rotation the greater the induced magnetic field.
- Increase in the magnetic field parameter reduces the induced magnetic field profiles. Increase in magnetic parameter leads to an increase in Lorentz forces which opposes the flow hence a decrease in the induced magnetic field.

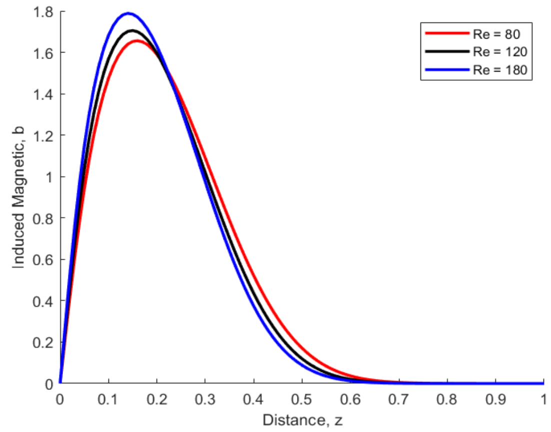

Fig. 23. Induced magnetic field and Reynolds number, R_e

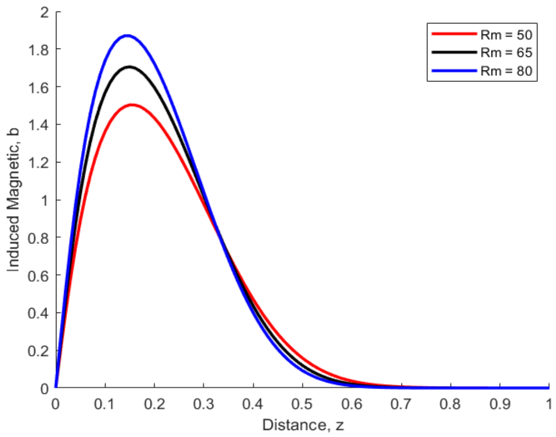

Fig. 24. Induced magnetic field and magnetic Reynolds number, R_m

From Fig. 23 & 24, we observe that;

- An increase in the magnetic Reynolds number, R_m and Reynolds number, R_e causes an increase in the induced magnetic field near the plate and decreases the induced magnetic field far away from the plate. This is due to the fact that presence of magnetic field acting perpendicular to the flow in an electrically conducting fluid produces a force which acts against the fluid flow.

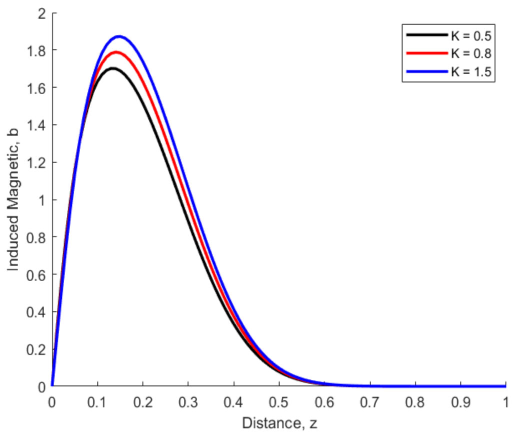

Fig. 25. Induced magnetic field and permeability parameter, K

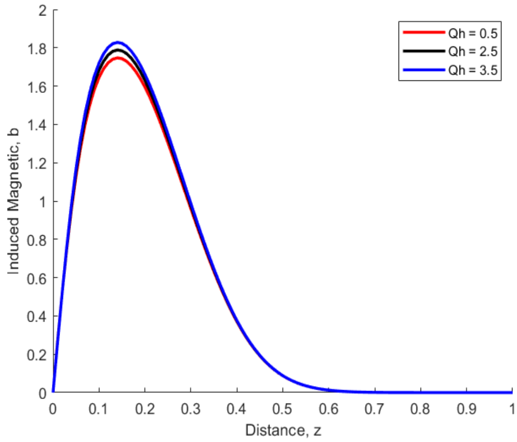

Fig. 26. Induced magnetic field and heat source parameter, Q_h

From Fig. 25 & 26, we observe that;

- An increase in the Permeability parameter, K causes an increase in the induced magnetic field near the plate and decreases the induced magnetic field far away from the plate.
- Heat source parameter induces eddy currents of the conducting fluid, hence increasing heat source parameter increases the induced magnetic field.

V. CONCLUSION

In this work the effects of induced magnetic field, and thermal diffusion past a semi- infinite porous plate with an oscillatory motion have been formulated and solved numerically. The finite difference method with the help of MATLAB software is adopted to solve the equations governing the flow. It is found that; increase in magnetic Reynolds number and Reynolds number causes an increase in the induced magnetic field and decreases the induced magnetic field far away from the plate. This leads to decrease in concentration due to increase in inertial forces hence an increase in temperature and velocity. However, increasing the rotation parameter increases the induced magnetic field which increases both primary and secondary velocities. Again, an increase the hall current parameter leads to an increase in both primary and secondary velocity profiles near the plate but the velocity remains constantly distributed far away from the plate. Again a decrease in suction increases temperature as well as concentration profiles.

From this observations, it's clear that the parameters in the governing equations affect velocity, temperature, concentration and induced magnetic profiles. It is recommended that this work can be extended by considering: variable strong magnetic field inclined at an angle to the plate, turbulent flow of nanofluid and also the effects of parameters in the governing equations on skin friction on both heat and mass transfer.

REFERENCES

[1] Choi, S. U., & Eastman, J. A. (1995). *Enhancing thermal conductivity of fluids with nanoparticles* (No. ANL/MSD/CP-84938; CONF-951135-29). Argonne National Lab.(ANL), Argonne, IL (United States).

[2] Sheri, S. R., & Modugula, P. (2017). Thermal-diffusion and diffusion-thermo effects on MHD flow through porous medium past an exponentially accelerated inclined plate with variable temperature. *ARPN Journal of Engineering and Applied Sciences*, *12*(19), 5518-5526.

[3] Vijaya Kumar, A. G., Veeresh, C., Varma, S. V. K., Umamaheswar, M., & Raju, M. C. (2017). Joule heating and thermal diffusion effects on MHD radiative and convective Casson fluid flow past an oscillating semi-infinite vertical porous plate. *Frontiers in Heat and Mass Transfer (FHMT)*, *8*.

International Journal of Novel Research in Interdisciplinary Studies
Vol. 10, Issue 2, pp: (1-15), Month: March – April 2023, Available at: www.noveltyjournals.com

[4] Reddy, P. C., Raju, M. C., Raju, G. S. S., & Reddy, C. M. (2017). Diffusion thermo and thermal diffusion effects on MHD free convection flow of Rivlin-Ericksen fluid past a semi- infinite vertical plate. *Bulletin of Pure & Applied Sciences-Mathematics and Statistics*, *36*(2), 266-284.

[5] Falodun, B. O., Onwubuoya, C., & Alamu, F. H. (2018). Magnetohydrodynamics (MHD) heat and mass transfer of Casson fluid flow past a semi-infinite vertical plate with thermophoresis effect: spectral relaxation analysis. In *Defect and Diffusion Forum* (Vol. 389, pp. 18-35). Trans Tech Publications Ltd.

[6] Sheikholeslami, M., Kataria, H. R., & Mittal, A. S. (2018). Effect of thermal diffusion and heat-generation on MHD nanofluid flow past an oscillating vertical plate through porous medium. *Journal of Molecular Liquids*, *257*, 12-25.

[7] Krishna, M. V. (2021). Radiation-absorption, chemical reaction, Hall and ion slip impacts on magnetohydrodynamic free convective flow over semi-infinite moving absorbent surface. *Chinese Journal of Chemical Engineering*.

[8] Ganapathy, R. (1994). A note on oscillatory Couette flow in a rotating system.

[9] Veera Krishna, M., Ameer Ahamad, N., & Chamkha, A. J. (2021). Hall Effects on Unsteady Magnetohydrodynamic Flow of a Nanofluid Past an Oscillatory Vertical Rotating Flat Plate Embedded in Porous Media. *Journal of Nanofluids*, *10*(2), 259-269.

[10] Das, S., Guchhait, S. K., Jana, R. N., & Makinde, O. D. (2016). Hall effects on an unsteady magneto-convection and radiative heat transfer past a porous plate. *Alexandria Engineering Journal*, *55*(2), 1321-1331.